JMEPEG (2011) 20:1289–1293
DOI: 10.1007/s11665-010-9748-4

1059-9495/$19.00

A Simple Relationship Between Axial and Torsional Cyclic Parameters

Jing Li, Zhong-ping Zhang, Qiang Sun, Chun-wang Li, and Rong-sui Li

(Submitted October 21, 2009; in revised form May 30, 2010)

The ultimate purpose of the present article is to theoretically estimate the cyclic shear strength coefficient and the cyclic shear strain hardening exponent. For this purpose, the relationship between axial and torsional cyclic parameters is addressed in light of the von-Mises criterion. Material data for 15 kinds of material have been taken from the technical literature to check the accuracy and reliability of the developed correlations. Maximum differences of 18.6 and 27.7% were observed for theoretical versus experimental results for the cyclic shear strength coefficient and the cyclic shear strain hardening exponent, respectively. Experimental verifications show that the devised relationship can describe the cyclic shear stress-strain curves well. The characteristic of the theoretical approach is simple and easy to use. In addition, the theoretical results can be further applied to examine the correctness of the test data.

Keywords cyclic shear strain hardening exponent, cyclic shear strength coefficient, cyclic strain hardening exponent, cyclic strength coefficient, theoretical estimation

1. Introduction

Fatigue analysis is very important in the design of mechanical structures and components. Fatigue properties of materials are essential for fatigue analysis. It is well known that the cyclic shear strength coefficient and the cyclic shear strain hardening exponent are two basic mechanical behavior performance parameters. When the fatigue properties of materials are being evaluated (Ref 1-3), it is necessary to know these two material constants. Even though these fatigue performance parameters can be determined experimentally, they are often calculated theoretically because comprehensive test data are not usually available. If reliable correlations with reasonable accuracy can be established, durability performance predictions and/or optimization analyses can be performed, while substantially reducing time and cost associated with material fatigue testing.

In general, the axial and torsional cyclic stress-strain curves can be expressed by the Ramberg-Osgood forms:

For uniaxial loading

$$\frac{\Delta\varepsilon}{2}=\frac{\Delta\sigma}{2E}+\left(\frac{\Delta\sigma}{2K'}\right)^{1/n'} \quad \text{(Eq 1)}$$

For torsional loading

$$\frac{\Delta\gamma}{2}=\frac{\Delta\tau}{2G}+\left(\frac{\Delta\tau}{2K'_{o}}\right)^{1/n'_{o}}, \quad \text{(Eq 2)}$$

where $\Delta\sigma$ and $\Delta\tau$ are the axial cyclic stress range and the cyclic shear stress range, respectively; $\Delta\varepsilon$ and $\Delta\gamma$ are the axial cyclic strain range and the shear cyclic strain range, respectively; K' and K'_{o} are the cyclic strength coefficient and the cyclic shear strength coefficient, respectively; n' and n'_{o} are the cyclic strain hardening exponent and the cyclic shear strain hardening exponent, respectively. E is the Young's modulus and G is the shear modulus.

As for the cyclic strength exponent and the cyclic strain hardening exponent, there are some methods have been developed to estimate these two cyclic parameters such as the method proposed by Zhang et al. (Ref 4). If a reliable relationship between the axial and torsional cyclic parameters

Jing Li, Z. Zhang, Qiang Sun, Chun-wang Li, and **Rong-sui Li**, The Science Institute, Air Force Engineering University, East Chang Le Road, Xi'an 710051, China. Contact e-mail: lijing02010303@163.com.

Nomenclature

E	Young's modulus
G	shear modulus
ψ	reduction in area (%)
	Poisson's ratio
$\Delta\varepsilon$	strain range in axial fatigue test
$\Delta\sigma$	stress range in axial fatigue test
$\Delta\gamma$	shear strain range in torsional fatigue test
$\Delta\tau$	shear stress range in torsional fatigue test
σ'_{f}	axial fatigue strength coefficient
ε'_{f}	axial fatigue ductility coefficient
b	axial fatigue strength exponent
c	axial fatigue ductility exponent
τ'_{f}	shear fatigue strength coefficient
γ'_{f}	shear fatigue ductility coefficient
b_{o}	shear fatigue strength exponent
c_{o}	shear fatigue ductility exponent
K'	cyclic strength coefficient
n'	cyclic strain hardening exponent
K'_{o}	cyclic shear strength coefficient
n'_{o}	cyclic shear strain hardening exponent

Subscript

t	the theoretical value

can be established, the two cyclic shear parameters can be estimated by using the cyclic axial ones. Therefore, in the present study, a simple relationship between the axial and torsional cyclic parameters is addressed in light of the von-Mises criterion. Experimental verifications by using 15 different materials show that the developed relationship can describe the cyclic shear stress-strain curves well.

2. Correlations Among Axial and Torsional Cyclic Parameters

The relationship between the applied strain amplitude and fatigue life under uniaxial loading and torsional loading can be expressed by Manson-Coffin equations: For uniaxial loading

$$\frac{\Delta\varepsilon}{2}=\frac{\sigma'_f}{E}(2N_f)^b+\varepsilon'_f(2N_f)^c \quad \text{(Eq 3)}$$

For torsional loading

$$\frac{\Delta\gamma}{2}=\frac{\tau'_f}{G}(2N_f)^{b_o}+\gamma'_f(2N_f)^{c_o} \quad \text{(Eq 4)}$$

The material constants σ'_f, ε'_f are the axial fatigue strength and ductility coefficient, respectively. b and c represent the axial fatigue strength and ductility exponent, respectively. The material constants, τ'_f and γ'_f, are the shear fatigue strength and ductility coefficient, respectively. b_o and c_o represent the shear fatigue strength and ductility exponent, respectively. The strain amplitudes of Eq 3 and 4 can be split into elastic and plastic components, and they can be individually related to life by equating to the first and second terms, respectively, on the right. Thus, Eq 3 and 4 can be rewritten as

$$\frac{\Delta\varepsilon_e}{2}=\frac{\sigma'_f}{E}(2N_f)^b \quad \text{(Eq 5)}$$

$$\frac{\Delta\varepsilon_p}{2}=\varepsilon'_f(2N_f)^c \quad \text{(Eq 6)}$$

and

$$\frac{\Delta\gamma_e}{2}=\frac{\tau'_f}{G}(2N_f)^{b_o} \quad \text{(Eq 7)}$$

$$\frac{\Delta\gamma_p}{2}=\gamma'_f(2N_f)^{c_o} \quad \text{(Eq 8)}$$

Similar to Eq 3 and 4, the strain amplitudes of Eq 1 and 2 can be split into elastic and plastic components as well. Thus, Eq 1 and 2 can be rewritten as

$$\Delta\sigma/2=E\Delta\varepsilon_e/2 \quad \text{(Eq 9)}$$

$$\Delta\sigma/2=K'\left(\Delta\varepsilon_p/2\right)^{n'} \quad \text{(Eq 10)}$$

and

$$\Delta\tau/2=G\Delta\gamma_e/2 \quad \text{(Eq 11)}$$

$$\Delta\tau/2=K'_o\left(\Delta\gamma_p/2\right)^{n'_o} \quad \text{(Eq 12)}$$

Combining Eq 5, 6, 9, and 10, it can be obtained that

$$E\Delta\varepsilon_e/2-K'\left(\Delta\varepsilon_p/2\right)^{n'}=0 \quad \text{(Eq 13)}$$

$$E\Delta\varepsilon_e/2-\left(\sigma'_f/\varepsilon'^{b/c}_f\right)\left(\Delta\varepsilon_p/2\right)^{b/c}=0 \quad \text{(Eq 14)}$$

Combining Eq 13 and 14, it can be obtained that

$$n'=b/c \quad \text{(Eq 15)}$$

$$K'=\sigma'_f/\varepsilon'^{b/c}_f \quad \text{(Eq 16)}$$

Similarly, the cyclic shear strength coefficient and cyclic shear strain hardening exponent can be expressed by

$$n'_o=b_o/c_o \quad \text{(Eq 17)}$$

$$K'_o=\tau'_f/\gamma'^{b_o/c_o}_f \quad \text{(Eq 18)}$$

In Ref (5), the equivalent stress (σ_{eq}) and strain (ε_{eq}) are defined by

$$\sigma_{eq}=\left(3/2s_{ij}s_{ij}\right)^{1/2} \quad \text{(Eq 19)}$$

$$\varepsilon_{eq}=\left(2/3e^e_{ij}e^e_{ij}\right)^{1/2}+\left(2/3\varepsilon^p_{ij}\varepsilon^p_{ij}\right)^{1/2}, \quad \text{(Eq 20)}$$

where s_{ij}, e_{ij}, and ε^p_{ij} are the deviatoric stress $\left(s_{ij}=\sigma_{ij}-\sigma_{kk}\delta_{ij}/3\right)$, the elastic deviatoric strain $\left(e^e_{ij}=\varepsilon^e_{ij}-\varepsilon^e_{kk}\delta_{ij}/3\right)$ and the plastic strain, respectively, and repeated indices imply summation over 1-3. δ_{ij} is the Kronecker δ. It is obtained that $\sigma_{eq}=\sigma$, $\varepsilon_{eq}=2(1+\nu)\varepsilon^e/3+\varepsilon^p$ for uniaxial loading (ε^e is the elastic strain and ε^p is the plastic strain), and $\sigma_{eq}=\sqrt{3}\tau$, $\varepsilon_{eq}=\gamma/\sqrt{3}$ for torsional loading. ν is the Poisson's ratio.

In light of the equivalent strain defined by Eq 20, 5, and 6 can be written as

$$\frac{\Delta\varepsilon_{eq,e}}{2}=\frac{2(1+\nu)\sigma'_f}{3\quad E}(2N_f)^b \quad \text{(Eq 21)}$$

$$\frac{\Delta\varepsilon_{eq,p}}{2}=\varepsilon'_f(2N_f)^c \quad \text{(Eq 22)}$$

In light of the effective strain amplitude (Eq 20), Eq 5 and 6 can be rewritten as

$$\frac{\Delta\varepsilon_{eq,e}}{2}=\frac{\tau'_f}{\sqrt{3}G}(2N_f)^{b_o} \quad \text{(Eq 23)}$$

$$\frac{\Delta\varepsilon_{eq,p}}{2}=\frac{\gamma'_f}{\sqrt{3}}(2N_f)^{c_o} \quad \text{(Eq 24)}$$

The relationship between E and G can be expressed as

$$G=E/2(1+\nu) \quad \text{(Eq 25)}$$

Combining Eq 21-25, and it can be obtained that

$$\tau'_f=\sigma'_f/\sqrt{3} \quad \text{(Eq 26)}$$

$$\gamma'_f=\sqrt{3}\varepsilon'_f \quad \text{(Eq 27)}$$

$$b_o=b \quad \text{(Eq 28)}$$

$$c_o=c \quad \text{(Eq 29)}$$

Substituting Eq 26-29 into Eq 17 and 18, it can be obtained as

$$n'_o=n' \quad \text{(Eq 30)}$$

$$K'_o = 3^{-\frac{1+n'}{2}} K' \quad \text{(Eq 31)}$$

It is worth mentioning here that the derivation (Eq 30 and 31) takes as their starting point the assumption that the material is isotropic. For anisotropic material such as textured sheet or drawn wire, the derived relationship may fail since the Young's modulus, E, depends on sample orientation. As many polycrystalline materials can be approximated as isotropic, the derivation can be used for these materials.

3. Experimental verifications

To check the accuracy and reliability of Eq 30 and 31, 15 different materials are selected from the technical literature (Ref 2, 5-10). The test data (K'_o and n'_o) are listed in Table 1 and 2. The results estimated by Eq 30 and 31 is tentatively denoted as $K'_{o,t}$ and $n'_{o,t}$, respectively. The relative deviations of them from the test ones are defined as $\delta K'_{o,t} = (K'_{o,t} - K'_o)/K'_o$, $\delta n'_{o,t} = \left(n'_{o,t} - n'_o\right)/n'_o$, respectively. The estimated shear cyclic parameters ($K'_{o,t}$ and n'_o) are compared with the experimental ones in Fig. 1. In this figure, the dashed lines indicated a factor of ±20% (in $K'_{o,t}/K'_o$ and $n'_{o,t}/n'_o$) scatter band. As can be seen from Fig. 1(a) and (b), Eq 30 and 31 give good estimation results for the investigated materials. In more detail, results listed in tables show $-18.3 < \delta K'_{o,t} < 18.6\%$ and $-20.4 < \delta n'_{o,t} < 27.7\%$. The absolute mean values $\overline{|\delta K'_{o,t}|}$ and $\overline{|\delta n'_{o,t}|}$ are 8.5 and 10.9%, respectively.

The cyclic shear strength coefficient and the cyclic shear strain hardening exponent list in tables are used in Eq 30 and 31, to develop the theoretical and the experimental cyclic shear stress-strain curves. These curves are shown in Fig. 2-5. In this figure, "—" and "…" correspond to (K'_o, n'_o) and ($K'_{o,t}$, $n'_{o,t}$), respectively. These figures show that Eq 30 and 31 can be used to estimate the cyclic shear strength coefficient and the cyclic shear strain hardening exponent. In addition, based on Eq 12, the following equation can be obtained:

$$\log(\Delta\tau/2) = \log K'_o + n'_o \log(\Delta\gamma_p/2) \quad \text{(Eq 32)}$$

It should be mentioned here that log $K'_o > 0$, while log $(\Delta\gamma_p/2) < 0$ in Eq 32. That is to say, when the sign of the $\delta K'_{o,t}$ is positive, the sign of the $\delta n'_{o,t}$ should be also positive to estimate the cyclic shear stress-strain curve well, and vice versa. Therefore, the difference between the theoretical cyclic shear stress-strain curve and the test curve not only depends on the values of $\delta K'_{o,t}$ and $\delta n'_{o,t}$, but also on the sign. When the signs are the same, the theoretical curves correlate well with the experimental ones. However, when the signs are not the same, the theoretical curves deviate greatly from the tested ones. For material FeE 460 steel, the ($\delta K'_{o,t}$, $\delta n'_{o,t}$) are (−18.3, 24.7), and for this material the signs is not the same.

Table 1 Theoretical prediction of the cyclic shear parameters (Ref 5)

Materials	SNCM630	SNCM439	SCM440	S45C	SCM435	SFNCM85S	SF60	S25C
E, GPa	196	208	204	206	210	201	208	209
σ'_f, MPa	1270	1380	1400	1400	1100	1040	978	821
ε'_f	1.54	1.89	0.675	0.449	0.996	0.316	0.187	0.216
b	−0.0732	−0.0722	−0.0879	−0.107	−0.067	−0.0924	−0.082	−0.0961
c	−0.823	−0.801	−0.650	−0.564	−0.708	−0.522	−0.439	−0.458
K', MPa	1060	1000	1040	1150	1070	1320	1350	1140
n'	0.054	0.066	0.094	0.152	0.089	0.180	0.186	0.210
K'_o, MPa	592	601	643	552	553	676	609	565
n'_o	0.050	0.072	0.108	0.119	0.085	0.173	0.156	0.199
$K'_{o,t}$, MPa	594	557	570	611	588	690	704	586
$\delta K'_{o,t}$, %	0.34	−7.3	−11.3	10.7	6.3	2.0	15.6	3.7
$n'_{o,t}$	0.054	0.066	0.094	0.152	0.089	0.180	0.186	0.21
$\delta n'_{o,t}$, %	8.0	−8.3	−12.9	27.7	4.7	4.0	19.2	5.5

Table 2 Theoretical prediction of the cyclic shear parameters (Ref 2, 6-10)

Materials	40CrNiMoA	AISI 304	Haynes 188	1045 HR	Inc 718	AISI 316	FeE 460
E, GPa	208	183	170.2	202	209	192.7	206
σ'_f, MPa	1081.6	1000	823	948	3950	1258.2	659.2
ε'_f	0.8312	0.171	0.489	0.26	1.50	0.121	0.5227
b	−0.0777	−0.114	−0.082	−0.092	−0.151	−0.097	−0.0588
c	−0.7320	−0.402	−0.73	−0.445	−0.761	−0.454	−0.5945
K', MPa	1073.7	1660	891	1258	1564	903.8	508
n'	0.103	0.287	0.113	0.208	0.0681	0.179	0.2161
K'_o, MPa	558.7	785	589	614	860	398.6	319
n'_o	0.103	0.296	0.142	0.217	0.079	0.169	0.1733
$K'_{o,t}$, MPa	586	819	484	648	869.8	472.9	260.5
$\delta K'_{o,t}$, %	4.9	4.3	−17.8	5.5	1.1	18.6	−18.3
$n'_{o,t}$	0.103	0.287	0.113	0.208	0.0681	0.179	0.2161
$\delta n'_{o,t}$, %	0.0	−3.0	−20.4	4.8	−13.8	5.9	24.7

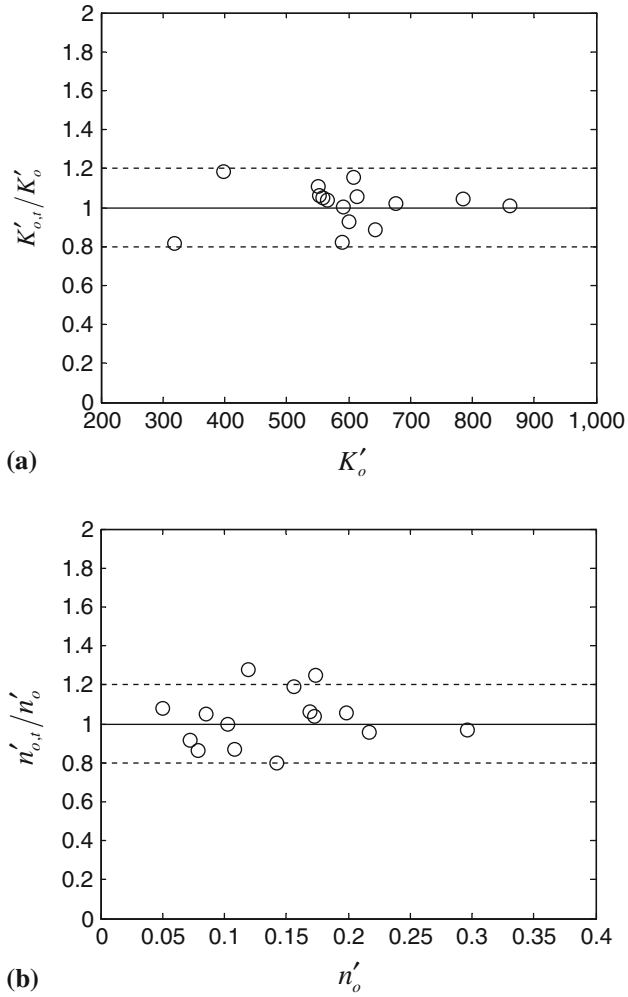

Fig. 1 Comparison of the estimated and experimental cyclic shear parameters (a) cyclic shear strength coefficient and (b) cyclic shear strain hardening exponent

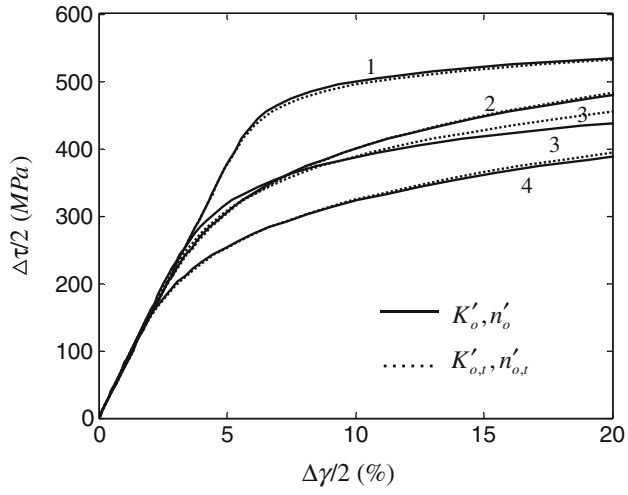

Fig. 2 Cyclic shear stress-strain curves for (1) SNCM630 steel (Ref 5), (2) SFNCM85S steel (Ref 5), (3) S45C steel (Ref 5), and (4) S25C steel (Ref 5)

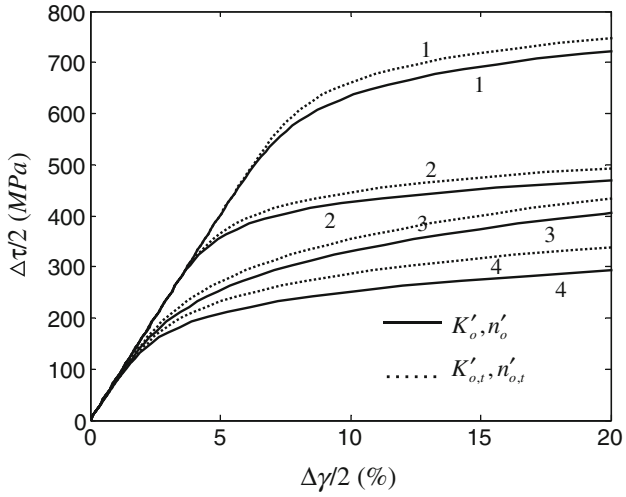

Fig. 3 Cyclic shear stress-strain curves for (1) Inc 718 (Ref 9), (2) SCM435 steel (Ref 5), (3) 1045 HR steel (Ref 9), and (4) AISI 316 (Ref 2)

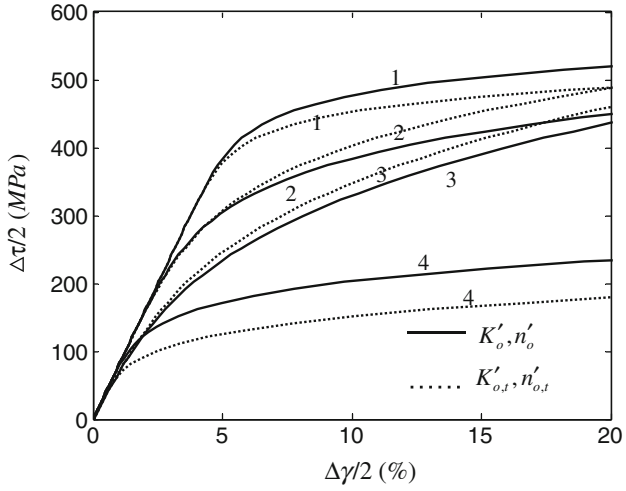

Fig. 4 Cyclic shear stress-strain curves for (1) SNCM439 steel (Ref 5), (2) SF60 steel (Ref 5), (3) AISI 304 (Ref 6), and (4) FeE 460 steel (Ref 10)

As such, the corresponding theoretical curves deviate greatly from the experimental one (Fig. 4).

The reasons why the FeE 460 steel behaves differently may be that the (K'_o, n'_o) itself is an experimental result, and there exists a difference between the test result and the theoretical one. What's more, the derivation based on the assumption that the equality of the plastic and elastic components in both Manson-Coffin equation and Ramberg-Osgood equation leads to the compatibility condition. In other words, the derivation assumed that the number of cycles to failure does not influence the elastic-plastic properties of the material. Thus, it is assumed that the material is stable during fatigue tests and does not exhibit significant softening or hardening effects. However, the FeE 460 steel exhibits significant cyclic softening character under the cyclic loading (Ref 10). This character may result in the deviation problem when the derived relationship is used to describe the torsional cyclic stress-strain curve.

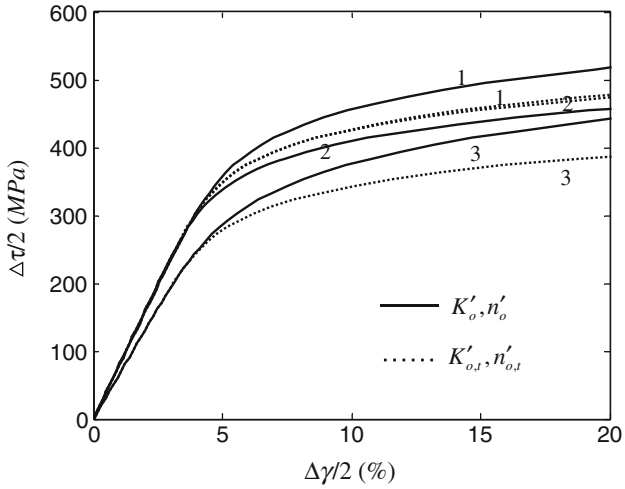

Fig. 5 Cyclic shear stress-strain curves for (1) SCM440 steel (Ref 5), (2) 40CrNiMoA steel (Ref 8), and (3) Haynes 188 (Ref 7)

4. Conclusions

Material data for 15 kinds of material published in Ref (2, 6-10) were used to examine correlations between the axial and torsional cyclic parameters. Based on the discussions in the preceding sections, the following conclusions can be drawn:

1. The cyclic shear strength coefficient is always less than the cyclic strength coefficient.
2. The cyclic strength coefficient and the cyclic strain hardening exponent can be used to estimate the cyclic shear strength coefficient and the cyclic shear strain hardening exponent. The expressions are as follows:

$$n'_o = n'$$

$$K'_o = 3^{-\frac{1+n'}{2}} K'$$

References

1. A. Fatemi and D.F. Socie, Critical Plane Approach to Multiaxial Fatigue Damage Including Out-of-Phase Loading, *Fatigue Fract. Eng. Mater. Struct.*, 1988, **11**(3), p 149–165
2. Y.M. Jen and W.W. Wang, Crack Initiation Life Prediction for Solid Cylinders with Transverse Circular Holes Under In-Phase and Out-of-Phase Multiaxial Loading, *Int. J. Fatigue*, 2005, **27**, p 527–539
3. C. Han, X. Chen, and K.S. Kim, Evaluation of Multiaxial Fatigue Criteria Under Irregular Loading, *Int. J. Fatigue*, 2002, **24**, p 913–922
4. Z.P. Zhang, Y.J. Qiao, Q. Sun et al., Theoretical Estimation to the Cyclic Strength Coefficient and the Cyclic Strain-Hardening Exponent for Metallic Materials: Preliminary Study, *J. Mater. Eng. Perform.*, 2009, **18**, p 245–254
5. K.S. Kim, X. Chen, C. Han, and H.W. Lee, Estimation Methods for Fatigue Properties of Steel Under Axial and Torsional Loading, *Int. J. Fatigue*, 2002, **24**, p 783–793
6. D.F. Socie, Multiaxial Fatigue Damage Models, *J. Eng. Mater. Technol.*, 1987, **109**, p 293–298
7. S. Kalluri and P.J. Bonacuse, In-Phase and Out-of-Phase Axial-Torsional Fatigue Behavior of Haynes 188 at 760°C, *Advances in Multiaxial Fatigue, ASTM STP, 1191*, D.L. McDowell and R. Ellis, Ed., American Society of Testing Materials, Cleveland, 1993, p 133–150
8. Z.L. Pu, K. Yang, and Z.D. Liu, An Experimental Study on Fatigue Behavior and Life Prediction Model of Coupling Bolt for the Steam Turbine, *Proc. CSEE*, 2002, **22**(7), p 90–94
9. A. Fatemi and P. Kurath, Multiaxial Fatigue Life Predictions Under the Influence of Mean Stresses, *J. Eng. Mater. Technol.*, 1988, **110**, p 380–388
10. C.M. Sonsino, Influence of Load and Deformation Controlled Multiaxial Tests on Fatigue Life to Crack Initiation, *Int. J. Fatigue*, 2001, **23**, p 159–167